

# Cell Number Quantification of USPIO-labeled Stem Cells by MRI: An *In Vitro* Study

Jerry S. Cheung<sup>1,2</sup>, April M. Chow<sup>1,2</sup>, Edward S. Hui<sup>1,2</sup>, Jian Yang<sup>1,2</sup>, Hung-Fat Tse<sup>5</sup>, \*Ed X. Wu<sup>1,2,3,4</sup>  
Department of Electrical and Electronic Engineering<sup>1</sup>, Laboratory of Biomedical Imaging and Signal  
Processing- 7T MRI Research Lab<sup>2</sup>, Medical Engineering Program<sup>3</sup>, The Jockey Club MRI Centre<sup>4</sup>,  
Department of Medicine<sup>5</sup>, The University of Hong Kong, Hong Kong SAR, China

\*Corresponding author: ewu@eee.hku.hk

**Abstract**—MRI plays an expanding role in stem cell therapies. The non-invasive nature and high spatial resolution of MR imaging make MR imaging a powerful tool to investigate biologic processes at the molecular and cellular level *in vivo* longitudinally. Quantitative detection of stem cells after transplantation may allow assessment of stem cell localization and migration, and monitoring of the therapeutic effectiveness of stem cell therapy. In this study, we present a technique for MR quantification of magnetically labeled mouse embryonic stem cells distributed or injected in agarose gel phantoms. Apparent transverse relaxation rate enhancements ( $\Delta R2^*$ ) were measured by gradient echo sequences. The linear relationship between  $\Delta R2^*$  and the concentration of USPIO-labeled mouse embryonic stem cells was observed and used for quantifying cell density and cell number after injection or transplantation. The MRI acquisition and analysis protocol were validated by good agreement between actual cell numbers and MRI-estimated cell numbers over a wide range of cell numbers. This MR technique for cell number and cell density quantification is applicable to future *in vivo* studies.

## I. INTRODUCTION

STEM cells can exhibit regenerative properties due to their plasticity, leading to the potential use of stem cells as therapeutic agents for repairing damaged organs and improving tissue function [1]. Most investigations have required the invasive analysis of interested organs postmortem. The non-invasive nature and high spatial resolution of MR imaging make MR imaging a powerful tool to investigate biologic processes at the molecular and cellular level *in vivo* longitudinally. After local grafting or systemic injection, transplanted stem cells may migrate from the site of transplantation or injection to relevant foci of disease. Magnetically labeled stem cells using MR contrast agents can be used to monitor the progression or repair of different ischemic diseases, such as myocardial infarction [2] and stroke [3, 4].

Superparamagnetic iron oxide (SPIO) nanoparticles and ultrasmall superparamagnetic iron oxide (USPIO) nanoparticles are negative MR contrast agents which reduce the signal intensity in T2-weighted or T2\*-weighted MR images due to magnetic susceptibility effect on the transverse relaxation. These nanoparticles have been used to monitor the migration of stem cells in different disease models [2, 3]. However, SPIO and USPIO nanoparticles cannot label stem cells or other mammalian cells efficiently in unmodified form.

Transfection agents such as poly-amines and lipids would coat with SPIO or USPIO nanoparticles via electrostatic interaction and chaperone these MR contrast agents into cells [5]. Transfection agents are highly charged macromolecules which form a complex stimulating endocytosis when combined with opposite surface charged SPIO or USPIO, thus facilitating the incorporation of the contrast agents into endosomes.

Although combining iron oxide nanoparticles with transfection agents offers a convenient way for MRI cell tracking, most MRI studies to date typically only involve implanting magnetically labeled cells into living subjects and tracking their movement and localization at specific tissues qualitatively without any quantification of cell number or cell density. Quantitative analysis of stem cell transplantation may allow assessment of stem cell localization and migration, and therefore the therapeutic effectiveness of the stem cell therapy. In addition, further optimization of stem cell therapy can be based upon the results of cell number and density quantification.

In this study, we present a technique for MR quantification of magnetically labeled mouse embryonic stem cells distributed or injected in agarose gel phantoms. Monocrystalline iron oxide nanoparticles (MION), one kind of USPIO, and Poly-L-lysine (PLL) are used. Apparent transverse relaxation rate enhancements ( $\Delta R2^*$ ) are found by gradient echo sequences. The relation between  $\Delta R2^*$  and cell concentration are investigated and used for cell number quantification. Good agreement between actual cell numbers and estimated cell numbers are found over a wide range of cell numbers.

## II. METHODOLOGY

### A. Cell Culture of Embryonic Stem Cells

Mouse embryonic stem (ES) cells (SCRC-1011, ATCC) were grown in DMEM media (Invitrogen) containing medium conditioned by mitotically-inactive mouse embryonic fibroblast (MEF) feeder cells (SCRC-1040, ATCC), 2mM L-glutamine (Invitrogen), 0.1mM non-essential amino acid (Invitrogen), 1mM sodium pyruvate, 20% ES Cell-Qualified Fetal Bovine Serum (Invitrogen), 100 $\mu$ M  $\beta$ -mercaptoethanol (Sigma), 10<sup>3</sup> units/ml leukemia inhibitory factor (Chemicon).

Mitotically-inactive MEF feeder layer was grown on a 10-cm tissue culture plate for one day. 10<sup>6</sup> R1 ES cells were grown on the MEF feeder layer in ES cell growth medium. The ES cell growth medium was changed daily, and R1 ES cells

were propagated when they reached 50-60% confluency. Medium was changed once two hours before trypsinization and 0.05% trypsin with 0.53 mM EDTA was used to detach ES cells from the plate, followed by centrifugation at 1,000 rpm for 5 minutes and dissociation into single cell by mechanical pipetting in growth medium. The suspended cells were adjusted to appropriate cell number (depends on days of culture) and then re-plated on a new mitotically-inactive MEF feeder layer for passage or on a 0.2% gelatin-coated plate before labeling.

### B. Magnetic Cell Labeling

The USPIO used in this study was MION-47 (stock concentration of 11.22 mg Fe/mL, Center for Molecular Imaging Research, MGH, Massachusetts) and the transfection agent (TA) used was Poly-L-lysine (PLL; average MW = 150-300 kDa, Sigma, St Louis, Mo), a polyamine.

For cell labeling, PLL of concentration 2.0  $\mu\text{g/mL}$  was mixed with MION-47 of concentration 50.0  $\mu\text{g/mL}$  for 60 minutes in cell culture medium at room temperature on a rotating shaker. These culture media were then added to the cells and kept overnight for about 24 hours at 37  $^{\circ}\text{C}$  in a 95% air per 5%  $\text{CO}_2$  atmosphere. Cells were washed twice with phosphate-buffered saline (PBS, pH = 7.4) to remove MION-TA complex, trypsinized, washed, and resuspended in 0.01 mol/L PBS at respective concentrations for phantom making. Viability was determined by Trypan blue exclusion three times and the result was expressed as percentage live cells of total cells. For Prussian blue staining, labeled cells were transferred to a microscope slide and fixed with 4% glutaraldehyde, washed, incubated for 30 minutes with 2% potassium ferrocyanide (Perls reagent) in 6% hydrochloric acid, washed again.

### C. MION Suspended Uniformly in Agarose Gel

Uniform gel suspensions (1% agarose gel) were prepared with MION concentrations of 0, 5.0, 10.0, 15.0, 20.0, 25.0, 30.0, 35.0, 40.0, 45.0, 50.0 and 55.0  $\mu\text{g/mL}$ , and placed in separate 4-cm long, 1-cm diameter cylindrical tubes. Apparent transverse relaxation rate ( $R2^*$ ) maps were computed from multi-echo gradient echo images at echo time (TE) = 8, 12, 16, 20, 24 ms with repetition time (TR) = 50 ms and flip angle (FA) = 30  $^{\circ}$  on a pixel-by-pixel basis. Values of  $\Delta R2^*$  of each tube with MION were calculated by subtracting  $R2^*$  of that tube by  $R2^*$  of tube without MION. Values of  $\Delta R2^*$  were then plotted against MION concentration and the relaxivity of MION-47 ( $\text{s}^{-1}/(\mu\text{g}\cdot\text{mL}^{-1})$ ), slope of the fitted line, was found for the estimation of cellular uptake of MION.

### D. Labeled Cells Suspended Uniformly in Agarose Gel

Uniform gel suspensions (1% agarose gel) were prepared with cell concentrations of 0,  $1.0\times 10^4$ ,  $5.0\times 10^4$ ,  $1.0\times 10^5$ ,  $2.5\times 10^5$ ,  $5.0\times 10^5$ ,  $7.5\times 10^5$ ,  $1.0\times 10^6$ ,  $2.0\times 10^6$ ,  $3.0\times 10^6$ ,  $4.0\times 10^6$  and  $5.0\times 10^6$  cells/mL, and placed in separate 4-cm long, 1-cm diameter cylindrical tubes.  $R2^*$  maps were computed from multi-echo gradient echo images at TE = 4, 8, 12, 16, 20 ms with TR = 50 ms and FA = 30  $^{\circ}$  on a pixel-by-pixel basis. Values of  $\Delta R2^*$  of each tube with labeled cells were calculated by

subtracting  $R2^*$  of that tube by  $R2^*$  of tube without cells. Values of  $\Delta R2^*$  were then plotted against cell concentration and the calibration constant  $C$  ( $\text{s}^{-1}/(\text{cells}\cdot\text{mL}^{-1})$ ), slope of the fitted line, was found for calibration in cell number quantification.

### E. Quantification of 5 $\mu\text{L}$ Labeled Cells injected in Agarose Gel

Different numbers of cells in 5 $\mu\text{L}$  of PBS from  $5.0\times 10^4$ ,  $7.5\times 10^4$ ,  $1.0\times 10^5$ ,  $2.5\times 10^5$ ,  $5.0\times 10^5$ ,  $7.5\times 10^5$  and  $1.0\times 10^6$  cells were injected into 3-mm circular holes in agarose gel in separate 4-cm long, 1-cm diameter cylindrical tubes, simulating *in vivo* situation.  $\Delta R2^*$  maps were computed from gradient echo images at TE = 1.94 ms with TR = 50 ms and FA = 30  $^{\circ}$  on a pixel-by-pixel basis as:

$$\Delta R2^* \approx -\frac{\ln(S_1/S_2)}{\text{TE}} \quad (1)$$

where  $S_1$  is the signal intensity of each pixel value in the image, and  $S_2$  is the mean of signal intensity of agarose gel. Estimated cell numbers (cells) were computed by the following equation:

$$\begin{aligned} \text{Estimated Cell Number} &= \iiint_V \frac{\Delta R2^*}{C} dV \\ &\approx \sum_i \frac{\Delta R2^*_i \cdot \Delta x \cdot \Delta y \cdot \Delta z}{C} \end{aligned} \quad (2)$$

where  $C$  is the calibration constant in unit of  $\text{s}^{-1}/\text{cells}\cdot\text{mL}^{-1}$ ,  $\Delta x\cdot\Delta y\cdot\Delta z$  is the reconstructed voxel size in unit of mL, and  $i$  is the slice number for which there is hypointensity in the image due to the labeled cells.

### F. MR Imaging and Data Analysis

All MR imaging was performed at 3.0 Tesla (Philips Intera Achiva) using a wrist coil. All cylindrical tubes were placed parallel to the main magnetic field. All T2\*-weighted images were acquired axially by 3D gradient echo sequence with field of view (FOV) = 77 mm, acquisition and reconstruction data matrix =  $128\times 128\times 32$  and  $256\times 256\times 32$  respectively. The final reconstructed resolution was  $0.3\times 0.3\times 0.6$  mm<sup>3</sup>. Images were analyzed using processing software developed at our laboratory using IDL (RSI, Boulder, CO, USA) programming language. Values of  $R2^*$  were calculated by linear least-squares fitting of log signal intensity versus echo time. The  $R2^*$  measurements were taken from three data samples of 3 contiguous slices by drawing circular region-of-interest (ROI) in the  $R2^*$  maps. The estimated cell numbers were taken from three measurements.

## III. RESULTS

### A. Cell Labeling

Prussian blue staining of cultured mouse embryonic stem cells and mouse fibroblasts labeled with MION-47 using PLL for 24 hours showed intracytoplasmic iron inclusions as dense blue-stained vesicles (Fig. 1a). None of the USPIO particles was seen inside the nucleus as demonstrated in the mouse embryonic fibroblast (*arrow*) which is consistent with other studies [6]. In contrary, no iron was detected in the control (Fig. 1b). Labeled mouse embryonic stem cell viability in culture after labeling, as determined by absence of uptake of Trypan blue stain, was  $92\pm 4\%$ .

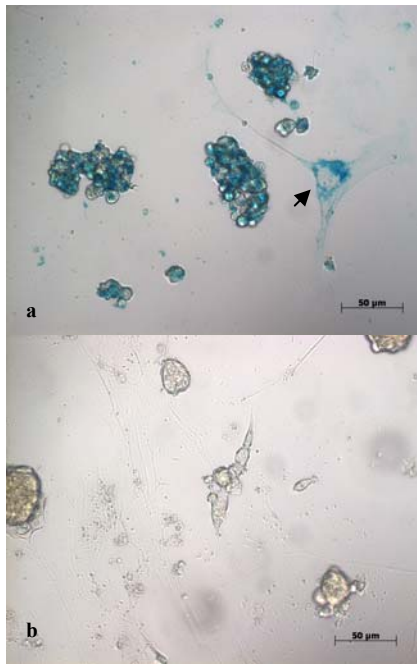


Fig. 1. Micrographs show a. clumps of mouse embryonic stem cells and mouse fibroblasts stained with Prussian blue to demonstrate the uptake of USPIO particles. USPIO particles are visible as blue iron deposits. No intranuclear uptake of USPIO could be observed in the fibroblast (*arrow*) b. mouse embryonic stem cells and fibroblasts without labeling of MION-PLL showing no apparent USPIO uptake.

### B. MION and Labeled Cells Suspended Uniformly in Agarose Gel

One of the slices of MION-47 suspended uniformly in agarose gel at TE = 16 ms and the corresponding R2\* map are shown in Fig. 2a and Fig. 2b respectively. Note that in Fig. 2a the first few phantoms except the first one (without MION) show hyperintensity, which is due to the T1-effect of MION at low concentration. However, the T1-effect is eliminated in the R2\* maps. Fig. 3 shows the plot of  $\Delta R2^*$  against MION concentration which corresponds well with theory that  $\Delta R2^*$  is approximately proportional to the concentration of contrast agent for gradient echo sequences [7]. The calculated relaxivity of MION-47 in 1% agarose gel is  $2.07 \text{ (s}^{-1}/(\mu\text{g}\cdot\text{mL}^{-1}))$ .

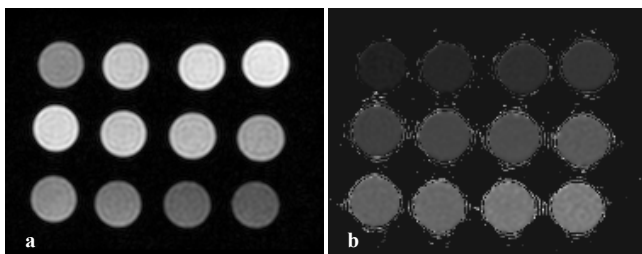


Fig. 2. a. Gradient echo image at TE = 16 ms of various concentration of MION suspended uniformly in agarose gel. b. The corresponding R2\* map. From left top to right bottom: 0, 5.0, 10.0, 15.0, 20.0, 25.0, 30.0, 35.0, 40.0, 45.0, 50.0 and 55.0  $\mu\text{g/mL}$

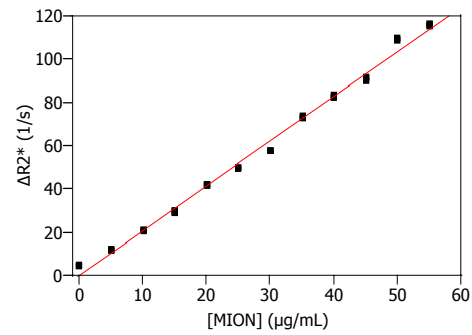


Fig. 3.  $\Delta R2^*$  versus MION concentration with fitted line  $\Delta R2^* = 2.07 [\text{MION}]$  and  $R^2 = 0.994$

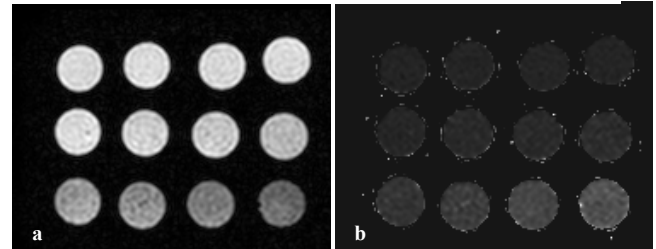


Fig. 4. a. Gradient echo image at TE = 16 ms of various concentration of cells suspended uniformly in agarose gel. b. The corresponding R2\* map. From left top to right bottom: 0,  $1.0 \times 10^4$ ,  $5.0 \times 10^4$ ,  $1.0 \times 10^5$ ,  $2.5 \times 10^5$ ,  $5.0 \times 10^5$ ,  $7.5 \times 10^5$ ,  $1.0 \times 10^6$ ,  $2.0 \times 10^6$ ,  $3.0 \times 10^5$ ,  $4.0 \times 10^5$  and  $5.0 \times 10^6$  cells/mL

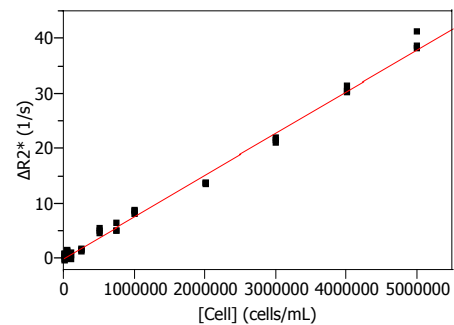


Fig. 5.  $\Delta R2^*$  versus cell concentration with fitted line  $\Delta R2^* = 7.65 \times 10^{-6} [\text{Cell}]$  and  $R^2 = 0.993$

One of the slices of labeled cells suspended uniformly in agarose gel at TE = 16 ms and the corresponding R2\* map are shown in Fig. 4a and Fig. 4b respectively. Fig. 5 shows the plot of  $\Delta R2^*$  against cell concentration. Despite the nature of inhomogeneous distribution of USPIO nanoparticles inside the cell as well as in the cell suspension, linear relationship is clearly seen for the cell concentration range studied. The slope or calibration constant  $C$  is  $7.65 \times 10^{-6} \text{ (s}^{-1}/\text{cells}\cdot\text{mL}^{-1})$  for the labeling procedure used in this study. Note that the calibration constant depends on the labeling protocol such as the type and concentration of contrast agent and transfection agent used, cell type and incubation time, and therefore should be different in different studies.

Based on the calibration curves in Figs. 3 and 5, the estimated cellular iron content for cells labeled using  $50 \mu\text{g/mL}$  of MION and  $2.0 \mu\text{g/mL}$  of PLL is about  $3.70 \text{ pg/cell}$ , assuming that both the MION and the labeled cells in agarose gel are randomly distributed and therefore have similar relaxivity.

### C. Cell Number Quantification

Contiguous slices which have hypointensity due to  $5.0 \times 10^5$  labeled cells injected in agarose gel are shown in Fig. 6. Table 1 shows the estimated cell number. Good agreement ( $R^2 = 0.955$ ) between actual cell numbers and estimated cell numbers are found for cell numbers from  $5.0 \times 10^4$  to  $1.0 \times 10^6$  cells (Fig. 7) with percentage (%) error ( $= 1 - \text{Estimated cell number} / \text{Actual cell number}$ ) from 1.31 % to 13.85 %. The error may be due to experimental error in making phantoms and computational error in the estimation of  $\Delta R2^*$  using Eq. 1.

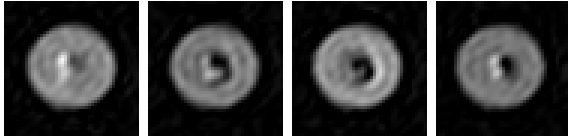


Fig. 6. Contiguous slices of gradient echo images at TE = 1.94 ms which show hypointensity due to  $5.0 \times 10^5$  labeled cells injected in agarose gel.

Cell Number (cells)				
Actual	50,000	75,000	100,000	250,000
Estimated	51,067	85,387	108,459	260,007
(N = 3)	$\pm 1,968$	$\pm 2,892$	$\pm 7,035$	$\pm 13,711$
% Error	2.13%	13.85%	8.46%	4.00%
Actual	500,000	750,000	1,000,000	
Estimated	543,502	740,138	948,300	
(N = 3)	$\pm 7,650$	$\pm 24,893$	$\pm 89,595$	
% Error	8.70%	1.31%	5.17%	

Table 1. Estimated cell number. The values shown are the mean  $\pm$  SD of three measurements

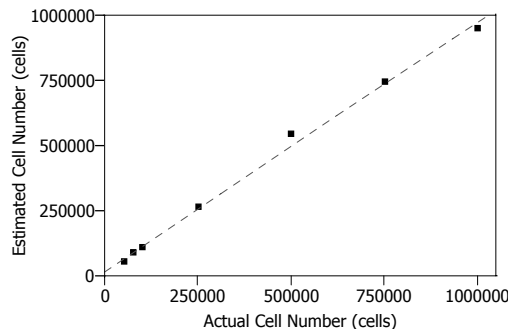


Fig. 7. Number of labeled cells injected in agarose gel phantoms estimated by MRI versus the actual cell number, with  $R^2 = 0.955$

## IV. CONCLUSIONS AND DISCUSSION

An MRI acquisition and analysis protocol to quantify the cell number of magnetically labeled cells were established and validated *in vitro*. Ultrasmall superparamagnetic iron oxide was used due to its high susceptibility effect on the transverse relaxation rate ( $R2^*$ ) and therefore high sensitivity on the quantification using  $\Delta R2^*$  [8]. The study has demonstrated good agreement between the actual cell numbers and the estimated cell numbers over a wide range of cell numbers. Mouse embryonic stem cells labeled with UPSIO using PLL as transfection agent were used in this study, showing a practical aspect of MR imaging technology in stem cell therapies.

The technique established here for cell number quantification is applicable to future *in vivo* studies provided

that the same stock of labeled cells is calibrated for its relaxation dependency on cell concentration. The possible limitations are: 1) error may arise from quantifying high number of cells in a small region, e.g., cell number  $> 2.0 \times 10^6$ , because the strong dephasing effect can lead to very low signal-to-noise ratio (SNR) in the raw images; 2) the relationship between  $\Delta R2^*$  and cell concentration may not be linear at high cell concentration, likely resulting in underestimation of cell number; 3) the quality of raw  $T2^*$  weighted images can affect the quantification accuracy. However, the technique proposed can be improved by acquiring the MR images of injected cells at very short TE, for example, by using projection reconstruction imaging, to increase the SNR of the images. Furthermore, by establishing the relationship between  $\Delta R2^*$  and cell density in high cell density range (likely non-linear [8]), the cell number measurement of high-density injections or distributions can be correctly calculated.

In conclusion, this study presents a MR technique for quantifying the number, density and distribution of labeled stem cells after injection or transplantation. Such technique is applicable and potentially valuable for monitoring and optimizing stem cell therapy *in vivo*.

## ACKNOWLEDGMENT

We thank the staff, especially Mr. Kevin Lai, in the Department of Medicine, Cardiology Division, LKS Faculty of Medicine, the University of Hong Kong, for technical assistance. This work was in part supported by the Hong Kong Jockey Club Charities Trust, The University of Hong Kong CRCG and Seeding Grants.

## REFERENCES

- [1] R. McKay, "Stem cells--hype and hope," *Nature*, vol. 406, pp. 361-4, 2000.
- [2] D. L. Kraitchman, A. W. Heldman, E. Atalar, L. C. Amado, B. J. Martin, M. F. Pittenger, J. M. Hare, and J. W. Bulte, "In vivo magnetic resonance imaging of mesenchymal stem cells in myocardial infarction," *Circulation*, vol. 107, pp. 2290-3, 2003.
- [3] M. Hoehn, E. Kustermann, J. Blunk, D. Wiedermann, T. Trapp, S. Wecker, M. Focking, H. Arnold, J. Hescheler, B. K. Fleischmann, W. Schwandt, and C. Buhle, "Monitoring of implanted stem cell migration in vivo: a highly resolved in vivo magnetic resonance imaging investigation of experimental stroke in rat," *Proc Natl Acad Sci U S A*, vol. 99, pp. 16267-72, 2002.
- [4] M. Modo, K. Mellodew, D. Cash, S. E. Fraser, T. J. Meade, J. Price, and S. C. Williams, "Mapping transplanted stem cell migration after a stroke: a serial, in vivo magnetic resonance imaging study," *Neuroimage*, vol. 21, pp. 311-7, 2004.
- [5] J. A. Frank, H. Zywicke, E. K. Jordan, J. Mitchell, B. K. Lewis, B. Miller, L. H. Bryant, Jr., and J. W. Bulte, "Magnetic intracellular labeling of mammalian cells by combining (FDA-approved) superparamagnetic iron oxide MR contrast agents and commonly used transfection agents," *Acad Radiol*, vol. 9 Suppl 2, pp. S484-7, 2002.
- [6] A. S. Arbab, G. T. Yocum, L. B. Wilson, A. Parwana, E. K. Jordan, H. Kalish, and J. A. Frank, "Comparison of transfection agents in forming complexes with ferumoxides, cell labeling efficiency, and cellular viability," *Mol Imaging*, vol. 3, pp. 24-32, 2004.
- [7] R. M. Weisskoff, C. S. Zuo, J. L. Boxerman, and B. R. Rosen, "Microscopic susceptibility variation and transverse relaxation: theory and experiment," *Magn Reson Med*, vol. 31, pp. 601-10, 1994.
- [8] E. X. Wu, H. Tang, and J. H. Jensen, "Applications of ultrasmall superparamagnetic iron oxide contrast agents in the MR study of animal models," *NMR Biomed*, vol. 17, pp. 478-83, 2004.